Accepted Manuscript Posted Online

JVI Accepted Manuscript Posted Online 30 March 2016
J. Virol. doi:10.1128/JVI.03267-15
Copyright © 2016, American Society for Microbiology. All Rights Reserved.

Mapping the specific amino acid residues to confer hamster DPP4 into a functional receptor for Middle East respiratory syndrome coronavirus

Neeltje van Doremalen[1], Kerri L. Miazgowicz[1]*, Vincent J. Munster[1]#

Laboratory of Virology, Division of Intramural Research, National Institute of Allergy and Infectious Diseases, National Institutes of Health, Hamilton, MT, USA[1]

Running Head: The molecular changes in hamster DPP4 to function as a receptor for MERS-CoV

#Address correspondence to Vincent J. Munster, vincent.munster@nih.gov

*Current affiliation: Department of Infectious Diseases, College of Veterinary Medicine, University of Georgia, Athens, GA, USA

Word count abstract: 73

Word count text: 1354

Journal of Virology
JVI
Journal of Virology

Accepted Manuscript Posted Online

Abstract

Novel emerging coronavirus MERS-CoV binds to its receptor dipeptidyl peptidase 4 (DPP4) via 14 interacting amino acids. We previously showed that if the five interacting amino acids which differ between hamster and human DPP4 are changed to its human residue, hamster DPP4 does act as a receptor. Here, we show that the functionality of hamster DPP4 as a receptor is severely decreased if less than four out of five amino acids are changed.

Importance

Novel emerging coronavirus MERS-CoV has infected >1600 people worldwide with a case fatality rate of ~36%. In this study we show that by changing four amino acids in hamster DPP4, this protein functions as a receptor for MERS-CoV. This work is vital in the development of new small animal models, which will broaden our understanding of MERS-CoV and be instrumental in the development of countermeasures.

Journal of Virology

JVI

Journal of Virology

Accepted Manuscript Posted Online

Journal of Virology

JVI

Journal of Virology

Introduction

Middle East respiratory syndrome coronavirus (MERS-CoV) has been detected in >1600 patients with a case-fatality rate of 36%. Although the majority of cases occurs in Saudi Arabia (80%), an outbreak in South Korea sparked by a patient with a travel history in the Middle East highlights the potential of MERS-CoV to transmit via the nosocomial route if no appropriate measures are taken (1). MERS-CoV has an unusual broad host tropism, including humans and dromedary camels. A better understanding of the molecular basis of the host tropism will help determine the restrictions of potential host species, improve the functional design of animal models and the development of medical countermeasures. Several animal models for MERS-CoV have been developed. Non-human primates (NHPs) (2-4) and dromedary camel models (5) are naturally susceptible. In addition, several mouse models have been developed, in which the expression of the human variant of the receptor of MERS-CoV, dipeptidyl peptidase 4 (DPP4), allows for viral replication (6-8). No other small animal models have been developed. Therefore, if a treatment is shown to be successful against MERS-CoV in the mouse model, further characterization of the treatment needs to be performed in NHPs, a relatively expensive model with limited accessibility. A second small animal model (such as hamsters with modified DPP4 (9, 10)) to confirm results obtained in the mouse model would ensure that only treatments with high likelihood of succeeding would be investigated in NHPs.

Fourteen amino acids (AA) are important in the interaction between blades IV and V of human DPP4 (hDPP4) and the receptor binding domain (RBD) of MERS-CoV spike protein (11, 12). We previously showed that hamster DPP4 (haDPP4) does not function as a receptor for MERS-CoV. This restriction is caused by five out of 14 interacting AAs which differ between hDPP4 and haDPP4 (*Figure 1*) (13). Here, we analyze the minimal combination of these five AAs allowing the haDPP4 to function as a receptor for MERS-CoV.

Materials and methods

Biosafety statement

All experiments performed with MERS-CoV were done in a high containment facility at the Rocky Mountain Laboratories (RML), Division of Intramural Research (DIR), National Institute of Allergy and

Accepted Manuscript Posted Online

Infectious Diseases (NIAID), National Institutes of Health (NIH). The work was approved by RML Institutional Biosafety Committee (IBC) at biosafety level 3 (BSL3).

Cells and virus

BHK (baby hamster kidney) were maintained in Dulbecco's modified Eagle's media (DMEM) supplemented with 10% fetal bovin serum (FBS), 2 mM L-Glutamine, 50 U/ml penicillin and 50 µg/ml of streptomycin (culture DMEM) and maintained at 37°C in 5% CO_2. MERS-CoV (strain HCoV-EMC/2012) was propagated on VeroE6 cells using DMEM supplemented with 2% FBS, 2 mM L-Glutamine, 50 U/ml penicillin and 50 µg/ml of streptomycin (complete DMEM). MERS-CoV was titrated by end-point titration in quadruplicate on VeroE6 cells cultured in complete DMEM as follows: cells were inoculated with ten-fold serial dilutions of virus, and scored for cytopathic effect 5 days later. $TCID_{50}$ was calculated by the method of Spearman-Karber (14).

Plasmids and transfection of BHK cells

Mutagenized DPP4 in expression plasmid pcDNA3.1(+) were generated using the Quickchange Lightning site-directed mutagenesis kit (Agilent). Modified DPP4 sequences were confirmed by Sanger sequencing. Baby hamster kidney cells were transfected with 3 µg pcDNA3.1(+) containing the DPP4 genes using 8 µl of Lipofectamine 2000 (Life Technologies). DPP4 expression was confirmed via flow cytometry.

Flow Cytometry

Transfected BHK cells were removed with 5 mM EDTA, resuspended in PBS with 2% FBS and stained at 4°C using α-human DPP4 antibody (R&D, AF1180), followed by staining with FITC-tagged donkey anti-goat antibody (Life technologies, A11055). As a control, samples of cells were stained with secondary antibody only. Only viable cells were selected using 7-amino actinomysin-D (Life Technologies). Samples were collected using a LSRII flow cytometer (BD Biosciences). 10,000 gated events were analyzed for each sample. Data were analyzed using FlowJo software (Treestar) comparing transfected BHK cells against untransfected BHK cells.

Journal of Virology
JVI
Journal of Virology

Accepted Manuscript Posted Online

Virus replication kinetics

Multistep replication kinetics were determined by inoculating cells with MERS-CoV with a multiplicity of infection (MOI) of 1 $TCID_{50}$ per cell. One hour after inoculation, cells were washed twice with DMEM and fresh complete DMEM was placed on the cells. Supernatants were sampled at 0, 24, 48 and 72 h after inoculation, and virus titers in these supernatants were determined as described. All experiments were done in triplicate. Mean viral titer and standard deviation were determined for each condition.

Image design

3D-images were created using PDB file 4KR0 and DPP4 sequence from GenBank file KF574266.1 in software Pymol v1.8 (15).

Results

The contribution of individual AAs was investigated by MERS-CoV infection of BHK cells transfected with haDPP4 containing single human AA substitutions (*Figure 2A*). None of the single mutant haDPP4 variants were able to support MERS-CoV replication. Next BHK cells were transfected with hDPP4 containing single hamster AA substitutions *(Figure 2B*). The substitutions A291E and R336T in hDPP4 abrogated MERS-CoV replication completely. AA substitution I295T reduced viral growth slightly compared to wildtype human DPP4. Expression of the other single AA substitutions (V341L and I346V) resulted in virus titers similar to BHK cells transfected with wildtype hDPP4. Then, three double mutants and one triple mutant were constructed with a backbone of haDPP4 and human AAs at the following positions; E291A and T295I; E291A and T336R; T295I and T336R; or E291A and T295I and T336R. Expression of these mutants on BHK cells did not result in MERS-CoV replication (*Figure 2C*). Finally, the functionality of haDPP4 with four out of five human residues was investigated. Attenuated MERS-CoV replication was measured when cells were expressing fully humanized haDPP4 but for residue 341V or 346I (*Figure 2D*).

Journal of Virology
JVI
Journal of Virology

Accepted Manuscript Posted Online

Discussion

We show that all of the five interacting residues that differ between hDPP4 and haDPP4 are important in binding of MERS-CoV spike protein. This is in contrast to murine DPP4, where mutagenesis of two out of five (L294A and R336T) interacting residues to human AAs resulted in MERS-CoV replication similar to hDPP4 (~1 log lower) (16).

Of the five residues important in haDPP4, 291 and 336 were found to be most critical, followed by residue 295, whereas 341 and 346 were found to be least critical. In hDPP4, residues A291, L294 and I295 form a hydrophobic core with RBD residues, surrounded by a hydrophilic periphery (11). In contrast, haDPP4 contains a hydrophilic residue at position 291 (E) and a neutral residue at position 295 (T), theoretically destroying the hydrophobic pocket. Indeed, residue E291 was found to be abortive in both backbones, whereas residue T295 has a moderate effect on RBD-DPP4 binding. Likewise, residue 295 was found to be less important in the binding of murine DPP4 by MERS-CoV RBD (17).

HaDPP4 is predicted to contain a glycosylation site at position 336, which is absent in hDPP4 and predicted to interfere with RBD binding (17). This is reflected in the observed lack of viral replication when DPP4 contains the hamster residue at position 336.

Finally, hDPP4 V341 and I346 form small hydrophobic patches with RBD residues, which are replaced with L341 and V346 in haDPP4. These residues have very similar properties to the residues in hDPP4 and result in a minimum attenuation. Although residues 341 and 346 have an effect on RBD binding in the background of haDPP4, this is much less critical than the interaction between RBD and residues 291, 295 and 336.

We observed a difference in outcome when using haDPP4 or hDPP4 as a backbone when investigating residues 295, 341 and 346; changes that have a negligible effect on hDPP4 and RBD binding can be measured as an attenuation in viral replication when using a haDPP4 background, reflecting suboptimal receptor binding.

In order to utilize the hamster as an animal model for MERS-CoV all five AAs involved in the host restriction need to be conferred to the hDPP4 equivalents in order to optimize the interaction between receptor and virus. Adaptation of MERS-CoV to haDPP4 is predicted to be unsuccessful, due to the glycosylation site at position 334-336. Transgenic hamsters are virtually absent from scientific literature

Journal of Virology JVI Journal of Virology

Accepted Manuscript Posted Online

due to the absence of specific gene targeting tools, utilization of the CRISPR/Cas9 system would allow efficient gene targeting and the generation of a new small animal model (9, 10).

Journal of Virology

JVI

Journal of Virology

Accepted Manuscript Posted Online

References

1. **WHO.** Middle East respiratory syndrome coronavirus. http://www.who.int/emergencies/mers-cov/en/. Accessed
2. **Falzarano D, de Wit E, Feldmann F, Rasmussen AL, Okumura A, Peng X, Thomas MJ, van Doremalen N, Haddock E, Nagy L, LaCasse R, Liu T, Zhu J, McLellan JS, Scott DP, Katze MG, Feldmann H, Munster VJ.** 2014. Infection with MERS-CoV causes lethal pneumonia in the common marmoset. PLoS Pathog **10:**e1004250.
3. **de Wit E, Rasmussen AL, Falzarano D, Bushmaker T, Feldmann F, Brining DL, Fischer ER, Martellaro C, Okumura A, Chang J, Scott D, Benecke AG, Katze MG, Feldmann H, Munster VJ.** 2013. Middle East respiratory syndrome coronavirus (MERS-CoV) causes transient lower respiratory tract infection in rhesus macaques. Proc Natl Acad Sci U S A **110:**16598-16603.
4. **Yao Y, Bao L, Deng W, Xu L, Li F, Lv Q, Yu P, Chen T, Xu Y, Zhu H, Yuan J, Gu S, Wei Q, Chen H, Yuen KY, Qin C.** 2014. An animal model of MERS produced by infection of rhesus macaques with MERS coronavirus. J Infect Dis **209:**236-242.
5. **Adney DR, van Doremalen N, Brown VR, Bushmaker T, Scott D, de Wit E, Bowen RA, Munster VJ.** 2014. Replication and shedding of MERS-CoV in upper respiratory tract of inoculated dromedary camels. Emerg Infect Dis **20:**1999-2005.
6. **Zhao J, Li K, Wohlford-Lenane C, Agnihothram SS, Fett C, Zhao J, Gale MJ, Jr., Baric RS, Enjuanes L, Gallagher T, McCray PB, Jr., Perlman S.** 2014. Rapid generation of a mouse model for Middle East respiratory syndrome. Proc Natl Acad Sci U S A **111:**4970-4975.
7. **Agrawal AS, Garron T, Tao X, Peng BH, Wakamiya M, Chan TS, Couch RB, Tseng CT.** 2015. Generation of a transgenic mouse model of Middle East respiratory syndrome coronavirus infection and disease. J Virol **89:**3659-3670.
8. **Pascal KE, Coleman CM, Mujica AO, Kamat V, Badithe A, Fairhurst J, Hunt C, Strein J, Berrebi A, Sisk JM, Matthews KL, Babb R, Chen G, Lai KM, Huang TT, Olson W, Yancopoulos GD, Stahl N, Frieman MB, Kyratsous CA.** 2015. Pre- and postexposure efficacy of fully human antibodies against Spike protein in a novel humanized mouse model of MERS-CoV infection. Proc Natl Acad Sci U S A **112:**8738-8743.
9. **Fan Z, Li W, Lee SR, Meng Q, Shi B, Bunch TD, White KL, Kong IK, Wang Z.** 2014. Efficient gene targeting in golden Syrian hamsters by the CRISPR/Cas9 system. PLoS One **9:**e109755.
10. **Gao M, Zhang B, Liu J, Guo X, Li H, Wang T, Zhang Z, Liao J, Cong N, Wang Y, Yu L, Zhao D, Liu G.** 2014. Generation of transgenic golden Syrian hamsters. Cell Res **24:**380-382.
11. **Lu G, Hu Y, Wang Q, Qi J, Gao F, Li Y, Zhang Y, Zhang W, Yuan Y, Bao J, Zhang B, Shi Y, Yan J, Gao GF.** 2013. Molecular basis of binding between novel human coronavirus MERS-CoV and its receptor CD26. Nature **500:**227-231.
12. **Wang N, Shi X, Jiang L, Zhang S, Wang D, Tong P, Guo D, Fu L, Cui Y, Liu X, Arledge KC, Chen YH, Zhang L, Wang X.** 2013. Structure of MERS-CoV spike receptor-binding domain complexed with human receptor DPP4. Cell Res **23:**986-993.
13. **van Doremalen N, Miazgowicz KL, Milne-Price S, Bushmaker T, Robertson S, Scott D, Kinne J, McLellan JS, Zhu J, Munster VJ.** 2014. Host species restriction of Middle East respiratory syndrome coronavirus through its receptor, dipeptidyl peptidase 4. J Virol **88:**9220-9232.
14. **Finney DJ.** 1964. Statistical method in biological assay. New York, Hafner Pub. Co.
15. **Schrödinger L.** The PyMOL Molecular Graphics System, v1.7.4.
16. **Cockrell AS, Peck KM, Yount BL, Agnihothram SS, Scobey T, Curnes NR, Baric RS, Heise MT.** 2014. Mouse dipeptidyl peptidase 4 is not a functional receptor for Middle East respiratory syndrome coronavirus infection. J Virol **88:**5195-5199.
17. **Peck KM, Cockrell AS, Yount BL, Scobey T, Baric RS, Heise MT.** 2015. Glycosylation of mouse DPP4 plays a role in inhibiting Middle East respiratory syndrome coronavirus infection. J Virol **89:**4696-4699.

Journal of Virology
JVI
Journal of Virology

Accepted Manuscript Posted Online

Acknowledgements

The authors would like to thank Drs. Bart Haagmans and Ron Fouchier for providing pcDNA3.1(+) human DPP4 and HCoV-EMC/2012, Rebekah McMinn and Jacob Conroy for assistance with the figures, and Aaron Carmody for assistance with the flow cytometry.

Funding

This research was supported by the Intramural Research Program of the National Institute of Allergy and Infectious Diseases (NIAID), National Institutes of Health (NIH).

Journal of Virology

JVI

Journal of Virology

Accepted Manuscript Posted Online

Table and Figures

Table 1. Summary of mutated DPP4 proteins and the ability to function as a MERS-CoV receptor

Backbone	Amino acid residue					Viral growth	$TCID_{50}$ at 72hpi
	291	295	336	341	346		
Human	**A**	**I**	**R**	**V**	**I**	+/+	8.1×10^4
Hamster	*E*	*T*	*T*	*L*	*V*	-/-	<DL
Hamster	**A**	*T*	*T*	*L*	*V*	-/-	<DL
Hamster	*E*	**I**	*T*	*L*	*V*	-/-	<DL
Hamster	*E*	*T*	**R**	*L*	*V*	-/-	<DL
Hamster	*E*	*T*	*T*	**V**	*V*	-/-	<DL
Hamster	*E*	*T*	*T*	*L*	**I**	-/-	<DL
Hamster	**A**	**I**	*T*	*L*	*V*	-/-	<DL
Hamster	**A**	*T*	**R**	*L*	*V*	-/-	<DL
Hamster	*E*	**I**	**R**	*L*	*V*	-/-	<DL
Hamster	**A**	**I**	**R**	*L*	*V*	-/-	5×10^0
Hamster	*E*	**I**	**R**	**V**	**I**	-/-	<DL
Hamster	**A**	*T*	**R**	**V**	**I**	-/-	<DL
Hamster	**A**	**I**	*T*	**V**	**I**	-/-	<DL
Hamster	**A**	**I**	**R**	*L*	**I**	+/-	2.4×10^3
Hamster	**A**	**I**	**R**	**V**	*V*	+/-	2.7×10^3
Human	*E*	**I**	**R**	**V**	**I**	-/-	<DL
Human	**A**	*T*	**R**	**V**	**I**	+/-	2.0×10^4
Human	**A**	**I**	*T*	**V**	**I**	-/-	<DL
Human	**A**	**I**	**R**	*L*	**I**	+/+	5.4×10^4
Human	**A**	**I**	**R**	**V**	*V*	+/+	7.7×10^4

Human residue = bold font; hamster residue = italic font; +/+ = viral growth; +/- = attenuated viral growth; -/- = no viral growth; <DL = below detection limit of the assay.

Journal of Virology
JVI
Journal of Virology

Accepted Manuscript Posted Online

Figure 1. Interaction between MERS-CoV RBD and DPP4. (A-F) Cartoon of detailed interactions between MERS-CoV residues and human (A-C) or hamster (D-F) DPP4 residues. (G-H) Cartoon of the predicted blockade of MERS-CoV RBD binding by glycosylation of motif 334-336 of hamster DPP4. DPP4 is depicted in green, MERS-CoV RBD is depicted in cyan, interacting AAs (A-F) or the glycosylation site (G-H) are depicted in grey.

Journal of Virology

JVI

Journal of Virology

Accepted Manuscript Posted Online

Figure 2. MERS-CoV replication in BHK cells expressing variants of DPP4. $TCID_{50}$ values were measured at 72 hpi. Number(s) below bars represent AA changed to human or hamster variant. (A) BHK cells were transfected with DPP4 of hamster origin with a single human AA mutation. (B) BHK cells were transfected with DPP4 of human origin with a single hamster AA mutation. (C) BHK cells were transfected with DPP4 of hamster origin with a double or triple human AA mutation. (D) BHK cells were transfected with DPP4 of hamster origin with a quadruple human AA mutation. Mean viral titers were calculated from three independent experiments. Error bars indicate standard deviations.

Journal of Virology
JVI
Journal of Virology

Accepted Manuscript Posted Online

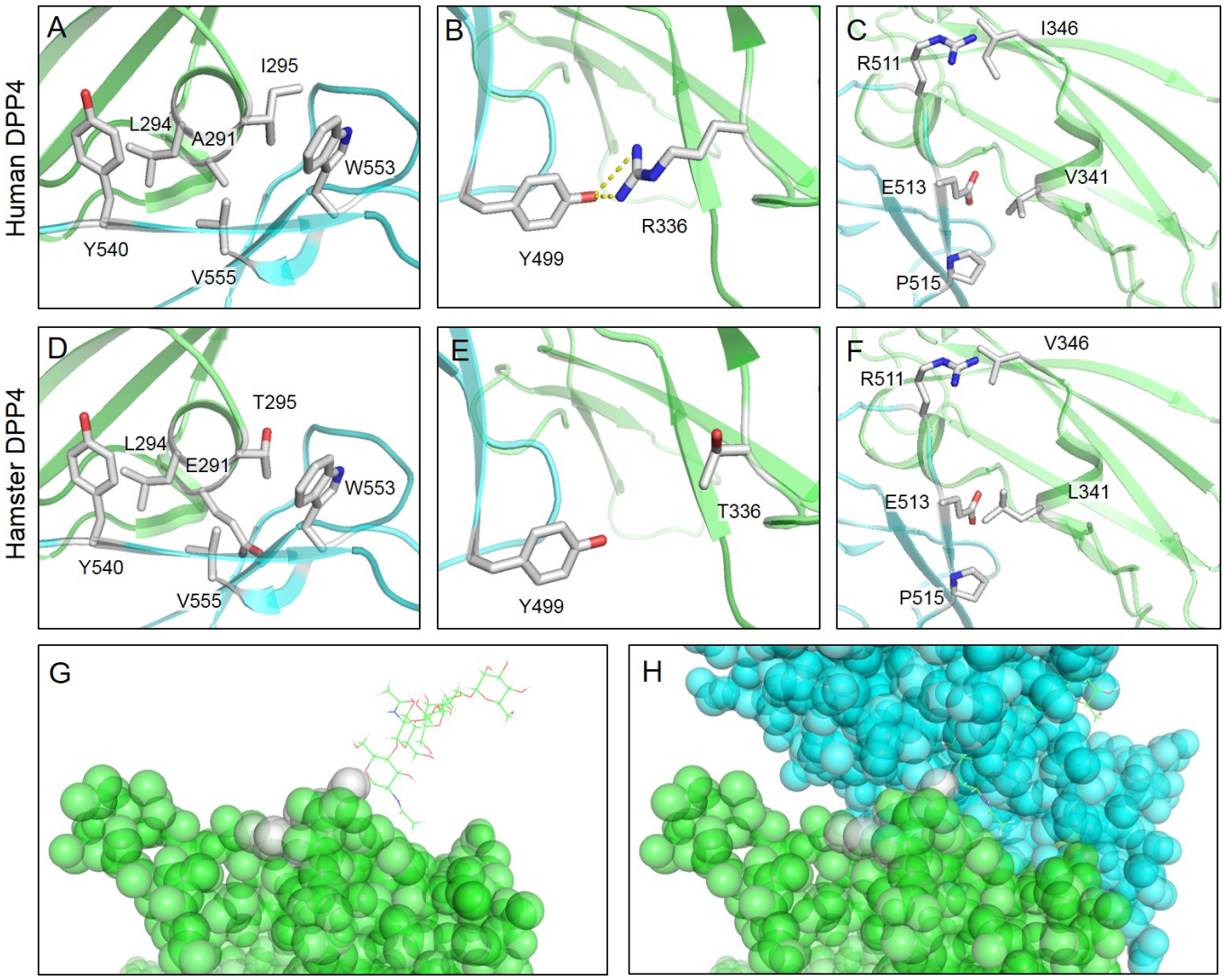

JVI Journal of Virology

Journal of Virology

Accepted Manuscript Posted Online

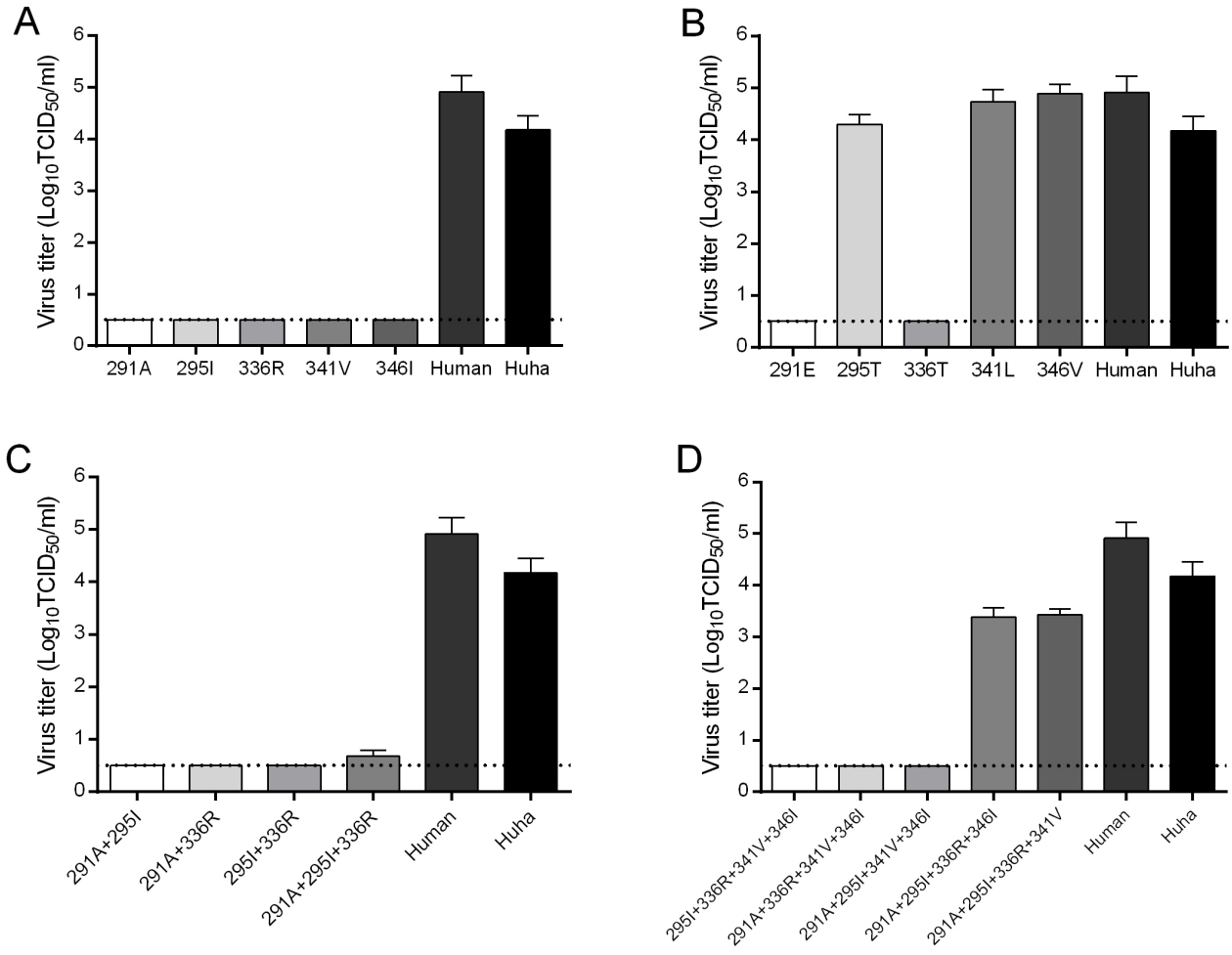

Journal of Virology
JVI
Journal of Virology